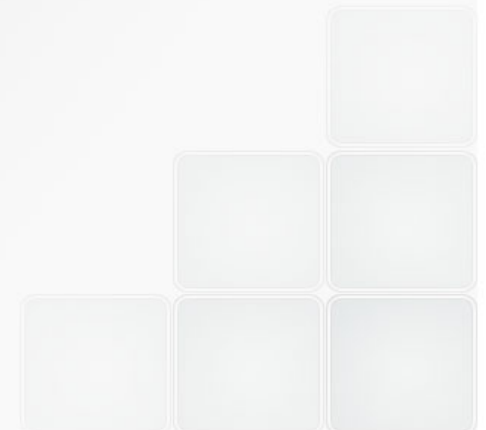




**ICTP IAEA School "Non-adiabatic
dynamics and radiation damage
in nuclear materials"
Trieste, 14-18 November 2011**

Applications of small-angle neutron scattering (SANS) in the micro- structural investigation irradiated nuclear steels

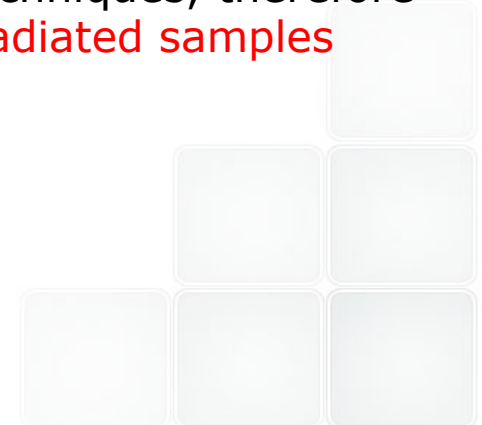
R. Coppola, ENEA-Casaccia



Cold neutron beams for fusion irradiated materials studies

Collimated beams of cold (25 meV) neutrons provide a unique experimental tool for microstructural investigation of irradiated fusion materials:

- They interact via the neutron scattering length parameter b varying randomly with Z and allowing to detect light elements like H ($b < 0$), He or Li and to distinguish for instance Fe and Cr
- Their absorption coefficient is much lower than for X-rays, allowing to investigate samples as thick as 1 mm or more, which is particularly suited for non-destructive stress investigation of TMB's and divertor prototypes
- Their magnetic moment allows to investigate magnetic materials
- No special metallurgical preparation is generally required and sample manipulation is considerably reduced with respect to other techniques, therefore **neutron scattering techniques are quite suitable for highly irradiated samples**



Major neutron sources



Australia

ANSTO - HIFAR Reactor (Sydney)

Canada

NRC Canadian Neutron Beam Centre, Chalk River

England

ISIS - Spallation Source, Rutherford –
Appleton Laboratory (Oxford)

France

LLB - Léon Brillouin Lab. at CEA (Saclay)
ILL- Grenoble

Germany

JCNS at FRM II
GKSS - Institute for Materials Research (Hamburg)
HZB - The Helmholtz Zentrum Berlin (HZB)

Japan

JAERI - Japan Atomic Energy Research Institute
KENS - High Energy Accelerator Organisation, KEK
KURRI - Research Reactor Institute (Kyoto)
JSNS - (part of the Japan proton accelerator research
complex (J-PARC)

Hungary

KFKI Research Institutes (Budapest)

Netherlands

RID - Reactor Institute Delft (RID), Delft University of Technology
HFR-JRC Petten

Russia

Frank Laboratory of Neutron Physics (JINR)
Joint Institute for Nuclear Research (Dubna)

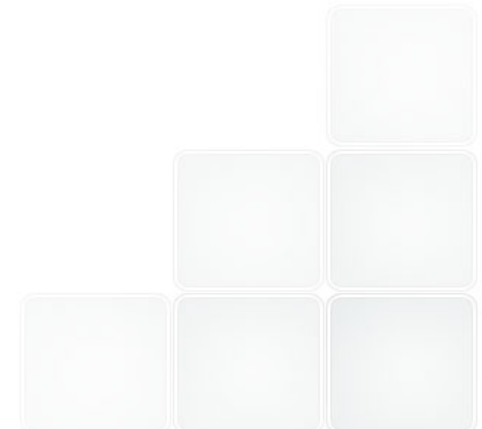
Switzerland

PSI - Paul Scherrer Institute

United States

LANSCCE - Los Alamos Neutron Science Center (Los Alamos)
NIST - Center for Neutron Research (Washington)
ORNL - High Flux Isotope Reactor (Oak Ridge)
SNS - Spallation Source, Oak Ridge

The European Spallation Source Lund (work in progress...)

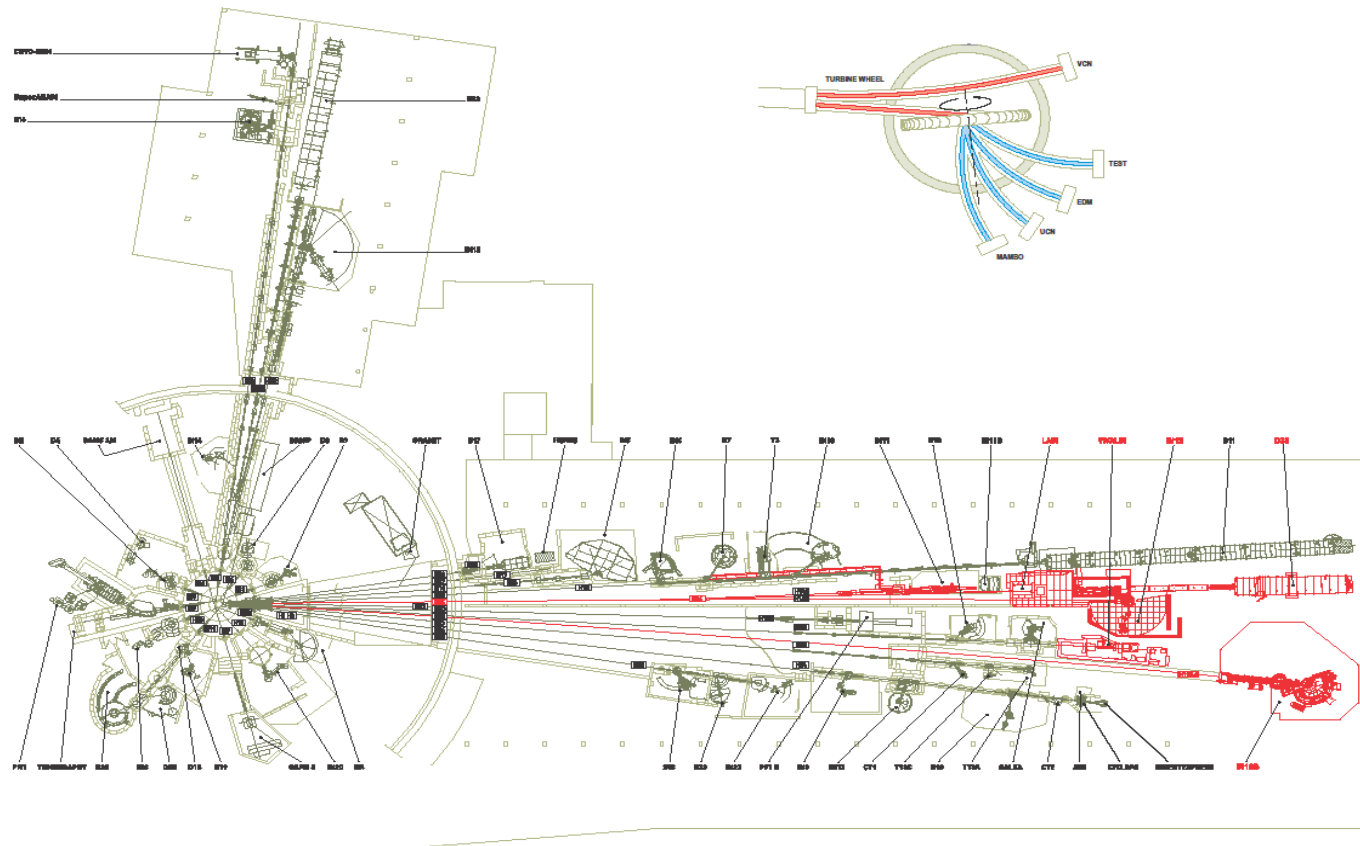




The 57 MW High Flux Reactor of the ILL-Grenoble, a partner of EIROforum organization

Flux 10^{15} n/s cm^2 thermal neutrons, available also for irradiation rigs

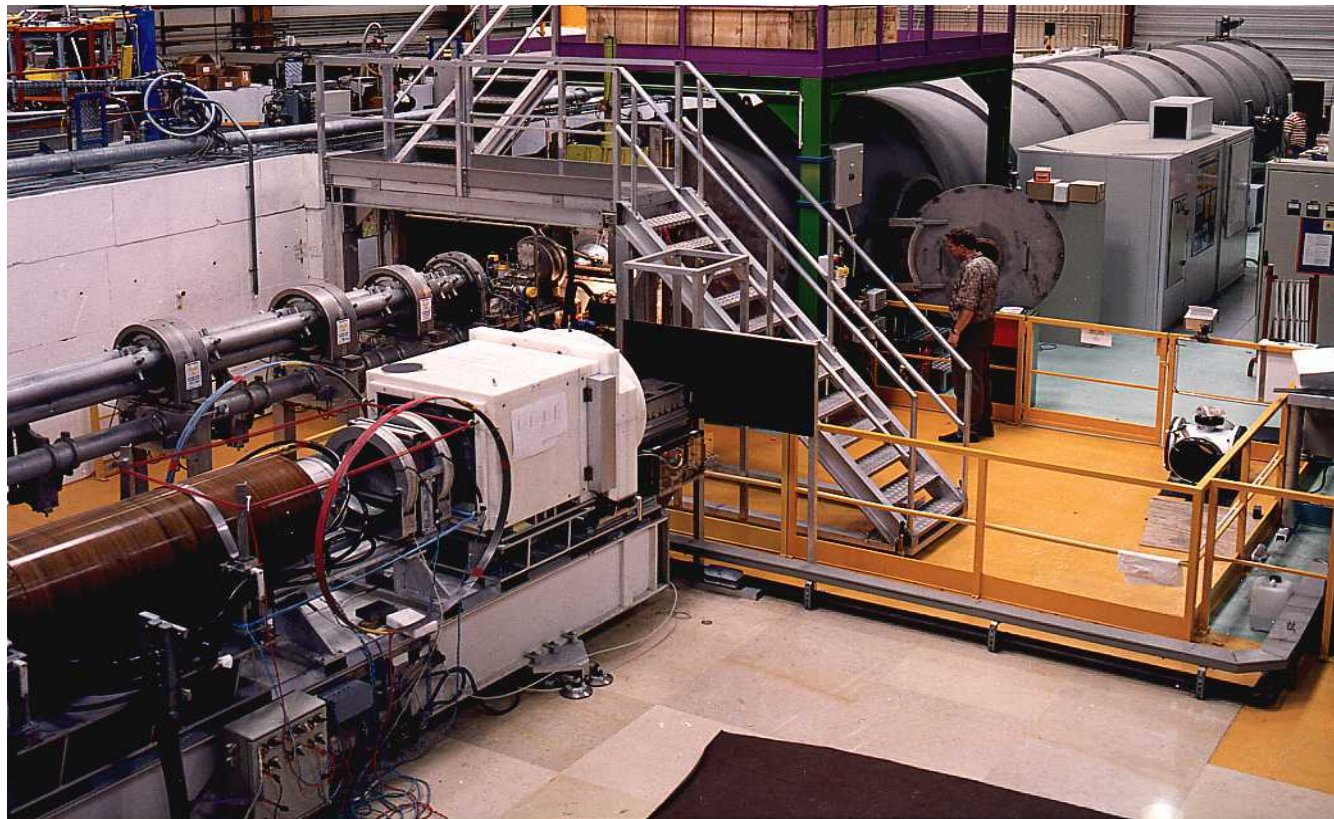
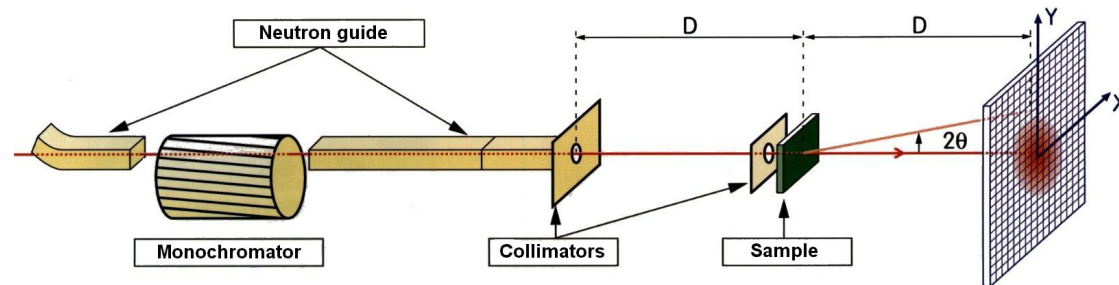




**Neutron guide halls, hosting 40 instruments in operation
(new in red)**

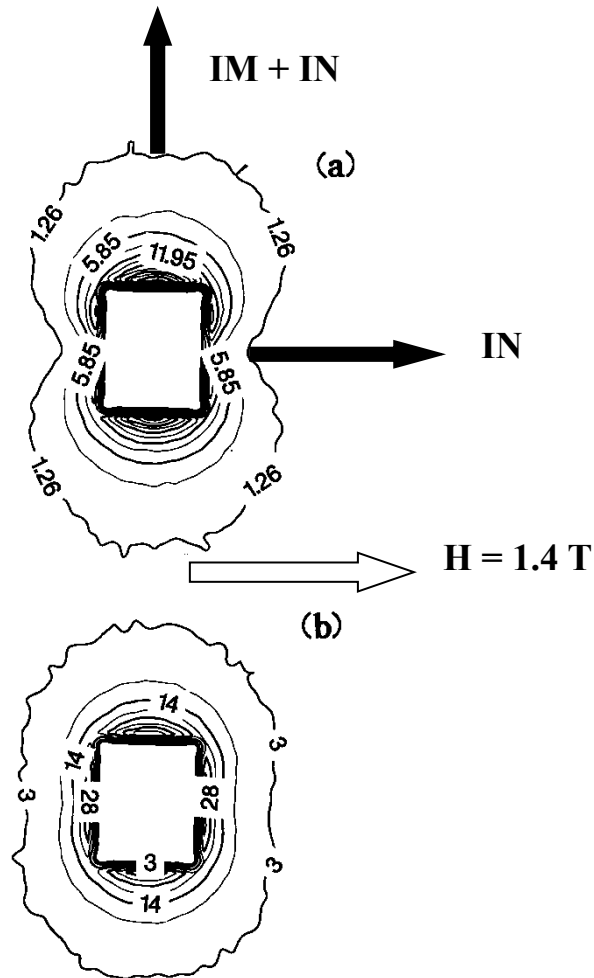


SANS instrument D22 at the ILL-Grenoble



Nuclear and magnetic SANS

Nuclear and magnetic SANS cross-section



a) reference sample, b) irradiated sample

$$\frac{d\Sigma(Q)}{d\Omega} = (\Delta\rho)^2 \int_0^\infty dR N(R) V^2(R) |F(Q, R)|^2$$

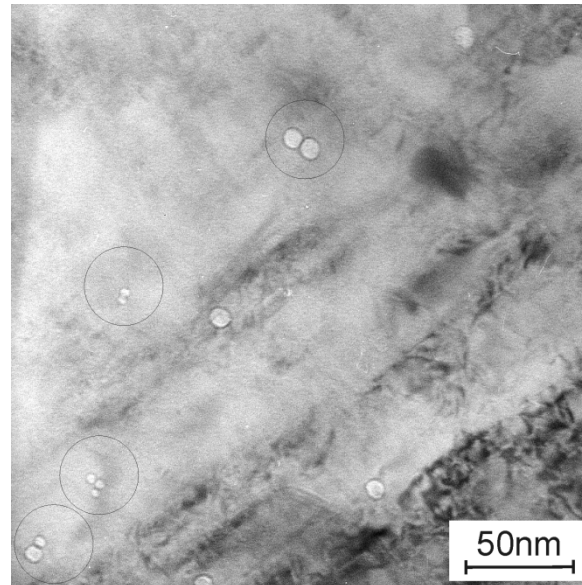
$$R(Q) = \frac{\frac{d\Sigma(Q)}{d\Omega_{nucl}} + \frac{d\Sigma(Q)}{d\Omega_{mag}}}{\frac{d\Sigma(Q)}{d\Omega_{nucl}}} = 1 + (\Delta\rho)_{mag}^2 / (\Delta\rho)_{nucl}^2$$

Polarised SANS

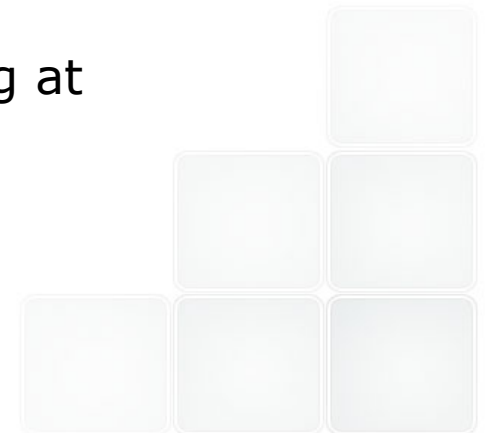
$$A_M \cdot A_N \propto \Delta\rho_m \cdot \Delta\rho_n$$



He bubbles in F82H-mod. steel implanted with α -particles at 250°C (400 appm) then annealed 2 h at temperatures between 550° C and 975 °C



Coalescence of helium bubbles after annealing at 975 °C (M. Klimiankou, FZK)

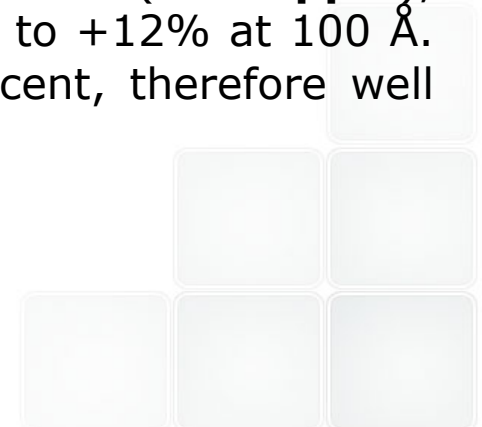


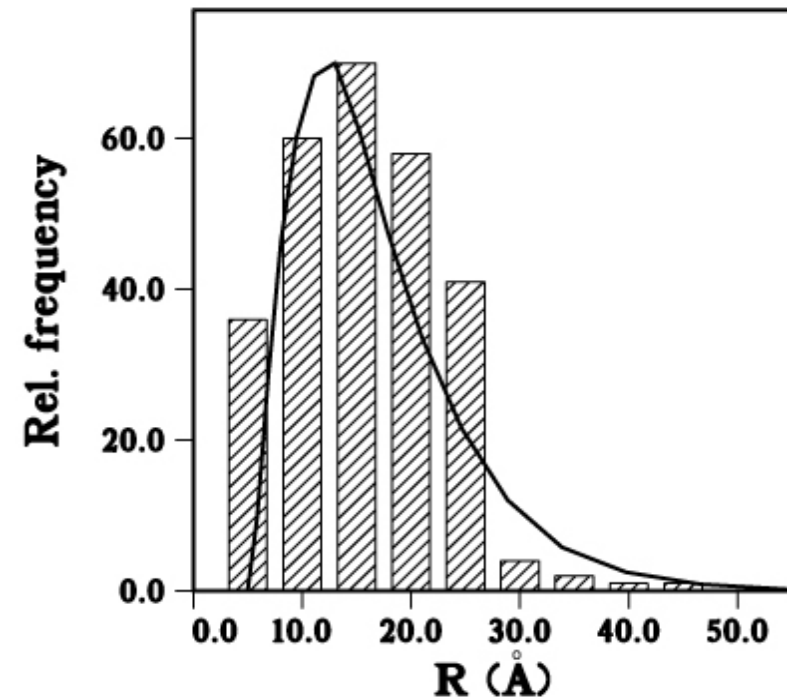
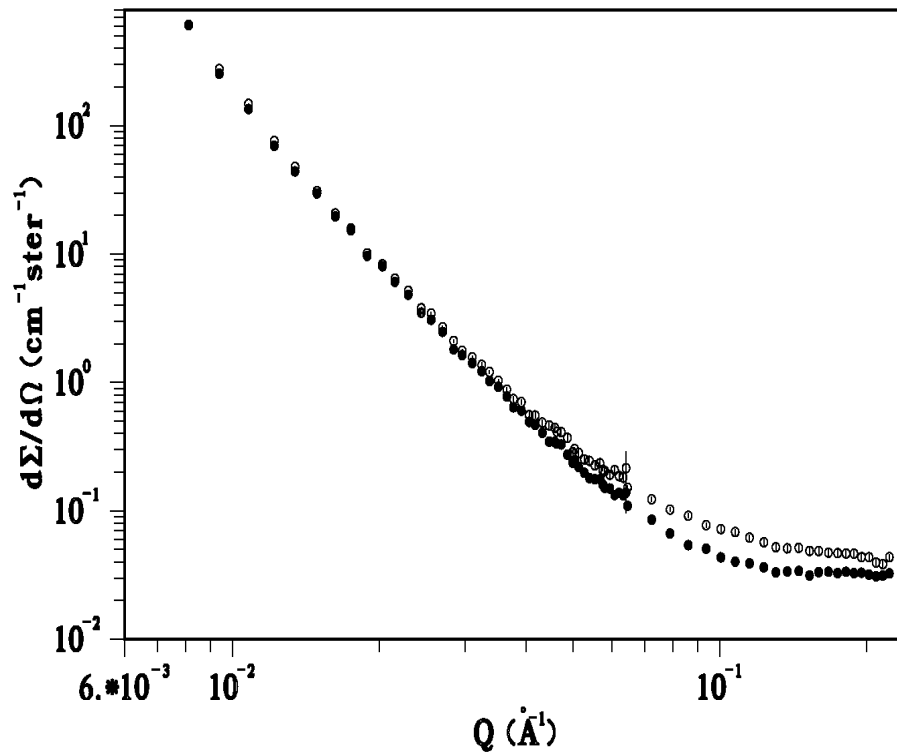
SANS contrast depends on bubble radius R

$$\Delta \rho (R) = \rho_{F82H} - b_{He} \rho_{He}(R)$$

$$C_{He} = v_M \int \rho_{He}(R) V(R) N(R) dR$$

The dependence of the contrast on the bubble radius is taken into account in the fitting procedure but given the small value of r_{He} very large changes of the He mass density would be necessary to lead to significantly different distributions. Assuming that the He concentration is equal to the nominal value (**400 appm**), the obtained variations on range typically from -10% at 2 Å to +12% at 100 Å. The resulting variations in $N(R)$ are generally of a few per cent, therefore well inside the statistical uncertainty band

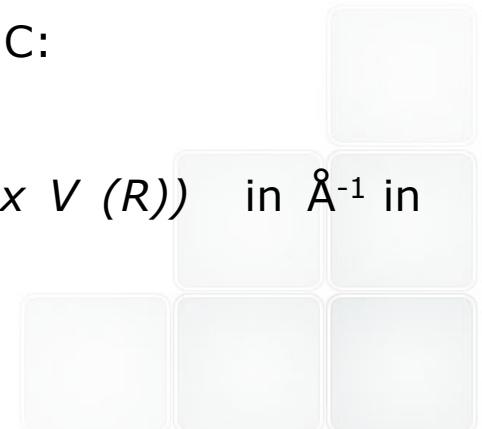




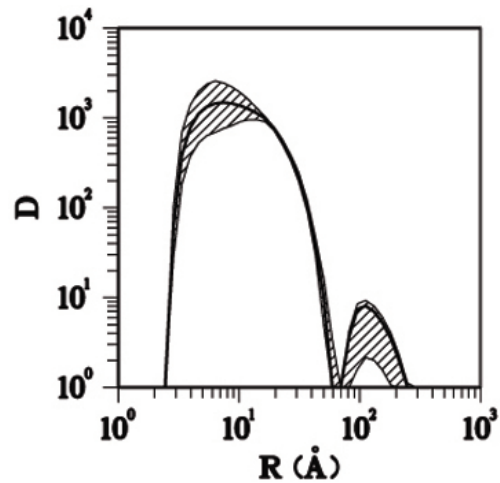
F82H-mod. steel as-implanted at 250°C then tempered at 825° C:

Left - SANS cross-sections of implanted and reference samples

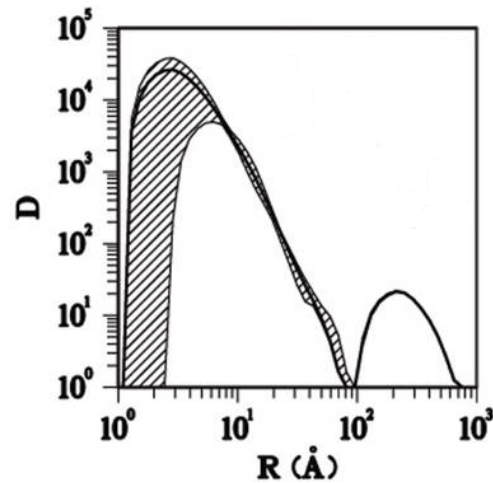
Right - best-fit He bubble volume distributions $D(R) (N(R) \times V(R))$ in \AA^{-1} in compared with the corresponding TEM histogram



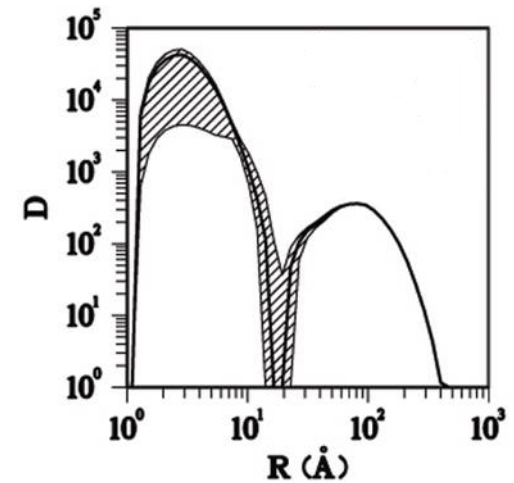
HELIUM BUBBLES VOLUME DISTRIBUTION IN F82H-mod.



250 °C

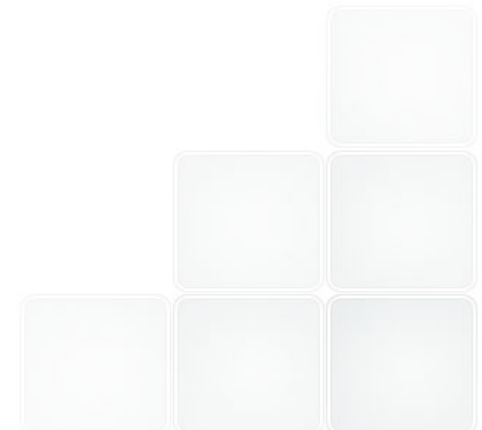


825 °C



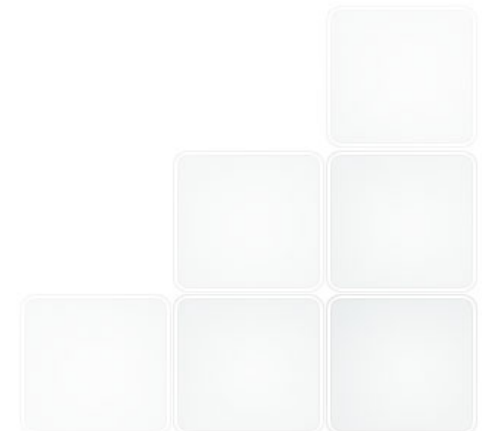
975 °C

The dashed area represents the 80% confidence band

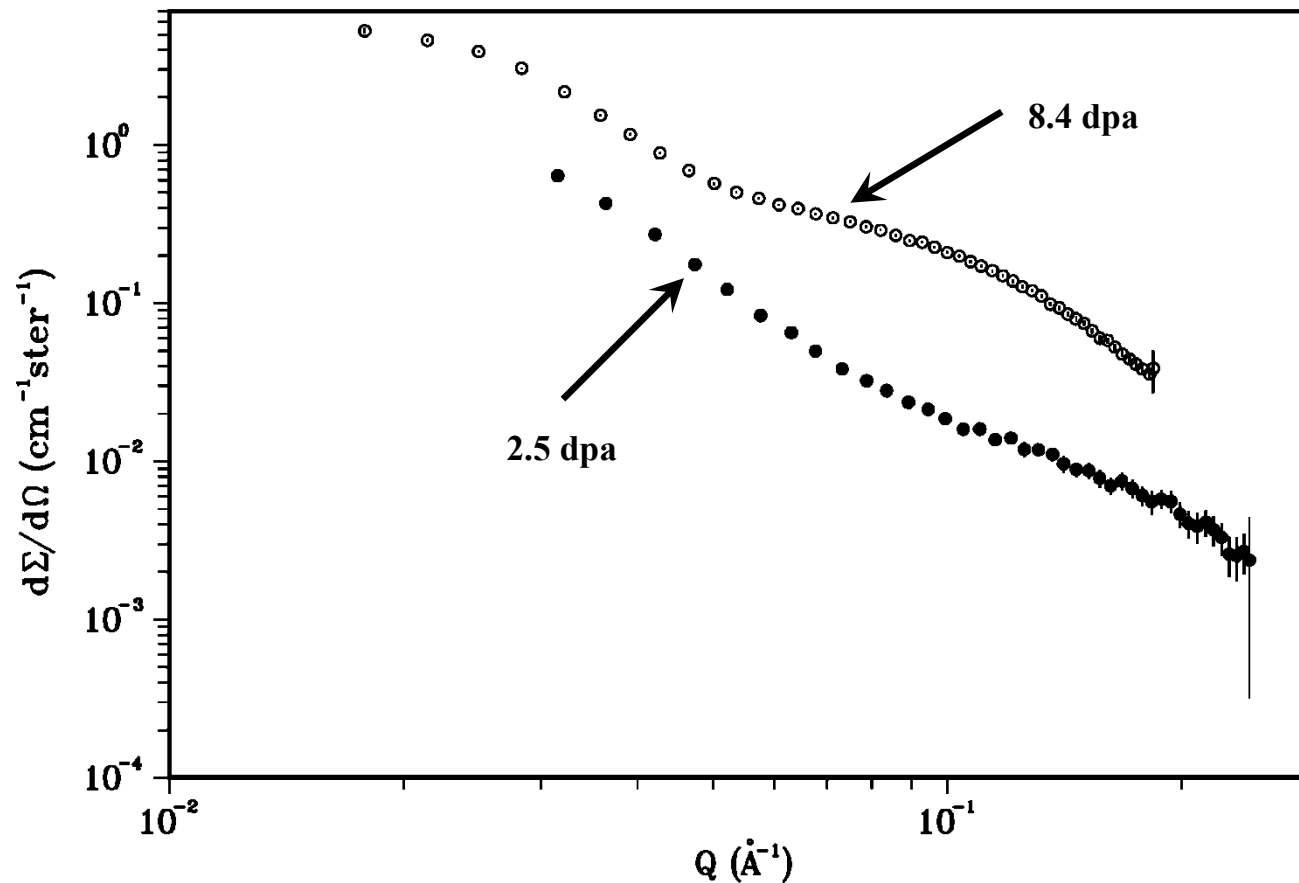


Best-fit helium bubble volume fraction, ΔV , helium concentration, C_{He} , and radii obtained from SANS data. The R and ΔV values in parentheses are those obtained from TEM.

Tempering Temperature	ΔV	$C_{He}(\text{appm})$	$R_V(\text{\AA})$
250 °C	0.0012 (0.0039)	209.0	11.1 (7)
825 °C	0.0053 (0.0036)	375.9	3.8 14.6 (17)
975 °C	0.0085 (0.0054)	558.9	4.1 45.9 (46)

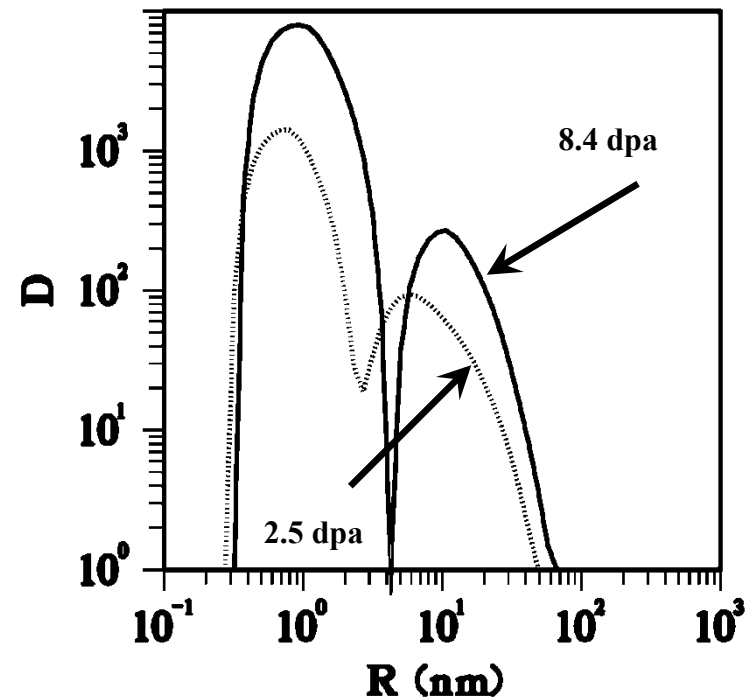


RESULTS ON 2.5 AND 8.4 dpa IRRADIATED EUROFER



Nuclear SANS cross-sections of the difference between Eurofer97 neutron irradiated at 250°C at **2.5 dpa** and at 300°C at **8.4 dpa** and their respective reference samples

MICROVOIDS EVOLUTION WITH IRRADIATION DOSE



Volume distribution functions $D(R)$ (nm^{-1}) obtained from the nuclear SANS difference between Eurofer97 neutron irradiated at 300°C and their respective reference samples (R. Coppola *et al.* J. Nuc. Mat. 386-388 (2009) 195)

Increasing the dose the average radius remains nearly unchanged but a consistent increase is observed in the volume fraction of the observed defects, from 0.005 at 2.5 dpa to 0.011 at 8.4 dpa

Polarised SANS



nuclear SANS cross-sections $(d\Sigma(Q)/d\Omega)_{nuc} = N^2$
magnetic SANS cross-section $(d\Sigma(Q)/d\Omega)_{mag} = M^2$
 α angle on the detector plane between Q and H

PSANS cross sections measured with spin parallel (+) and antiparallel (-) to H :

$$(d\Sigma(Q)/d\Omega)_{\pm} = N^2 \pm 2NM\sin\alpha + M^2\sin^2\alpha$$

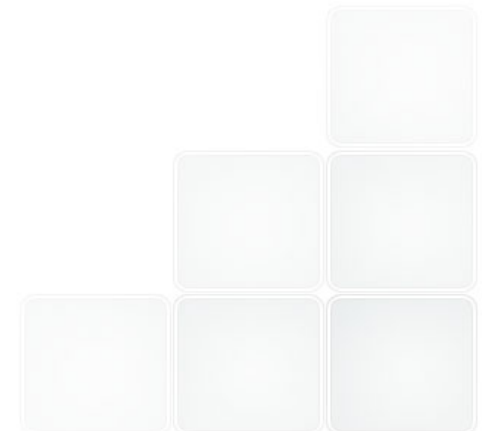
for $\alpha = 90^\circ$:

$$((d\Sigma(Q)/d\Omega)_{+} + (d\Sigma(Q)/d\Omega)_{-})/2 = N^2 + M^2$$

$$((d\Sigma(Q)/d\Omega)_{+} - (d\Sigma(Q)/d\Omega)_{-})/2 = 2NM \Rightarrow (\Delta\rho)_n(\Delta\rho)_m$$

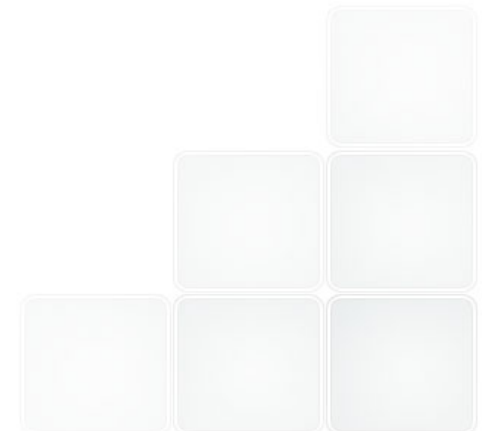
For $\alpha=0^\circ \rightarrow N$ then:

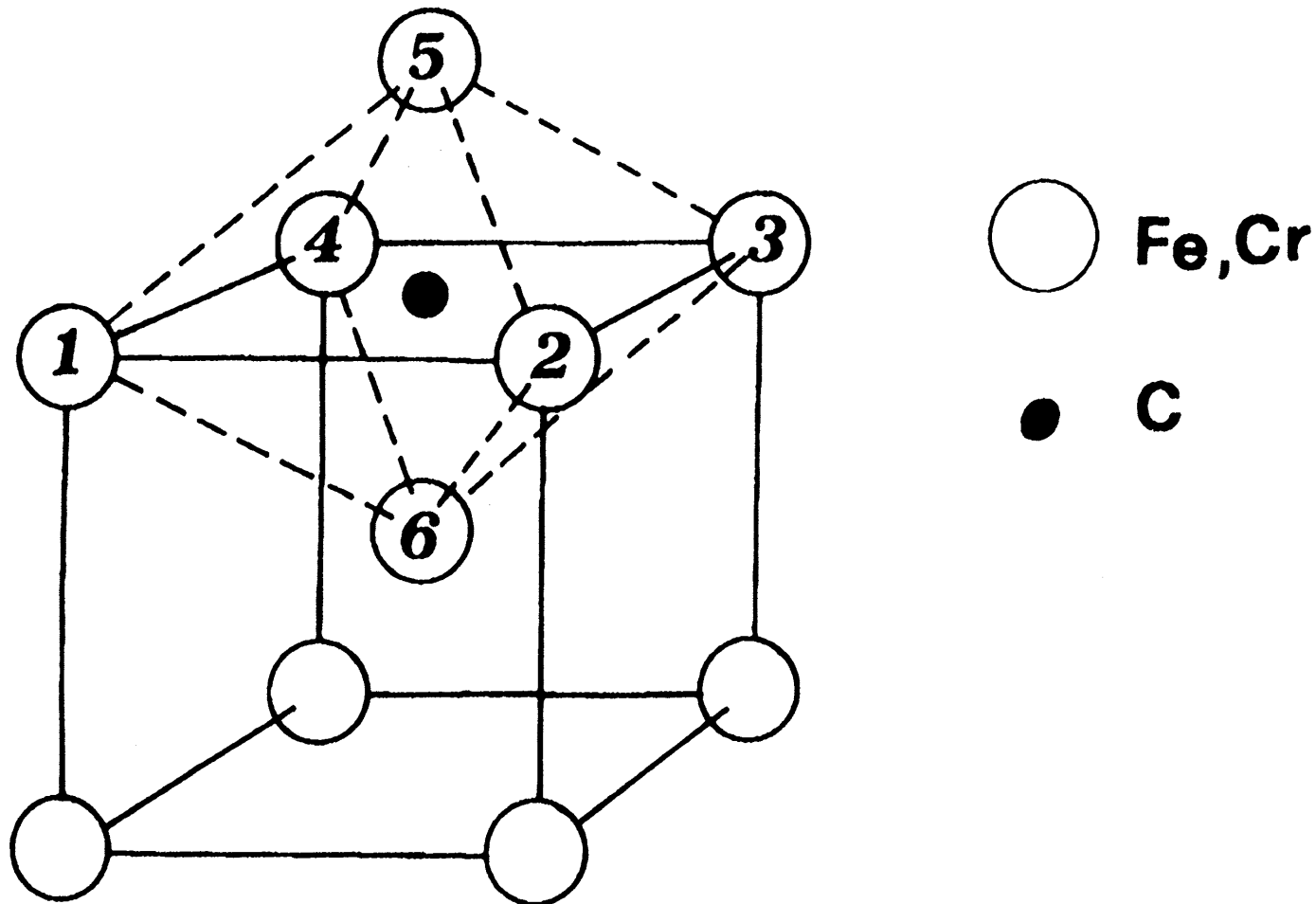
$$R(Q) = (N^2 + M^2)/N^2 = 1 + (\Delta\rho)_m^2 / (\Delta\rho)_n^2$$



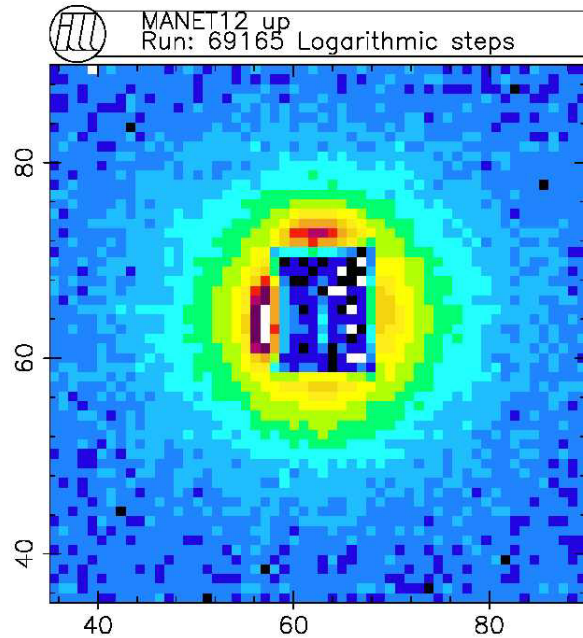
Polarised SANS using D22 at ILL

- magnetic field (1 T) perpendicular to the neutron beam path
- multilamellar deflecting supermirror to polarise the neutron beam and a spin-flipper to reverse the spin direction (flipping ratio near 40)
- $\lambda = 6 \text{ \AA}$ and $D = 2 \text{ m}$ were used, with Q-values ranging between $2 \cdot 10^{-2} \text{ \AA}^{-1}$ and $2 \cdot 10^{-1} \text{ \AA}^{-1}$ approximately ($Q = (4\pi\sin\theta)/\lambda$ where 2θ is the full scattering angle)

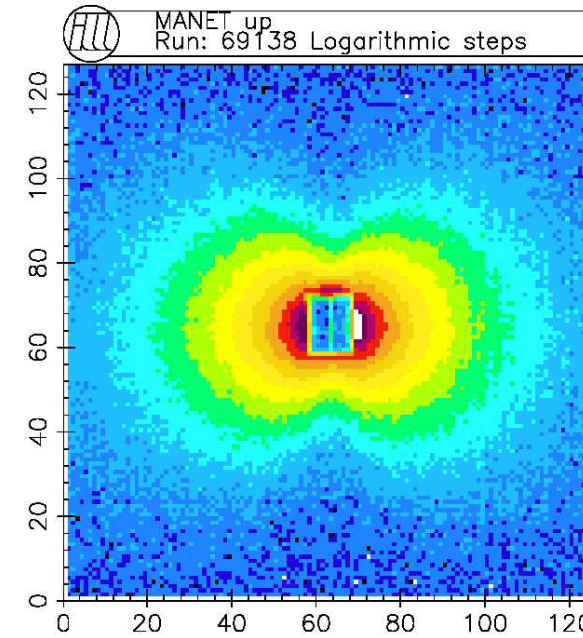




The bcc lattice cell of MANET steel with an interstitial C atom in octahedral position; the six nearest neighbours can be Fe atoms or a number of Cr ones varying between 1 and 6 for the different thermal treatments

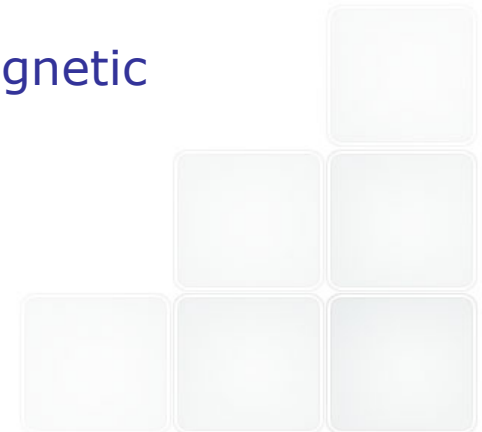


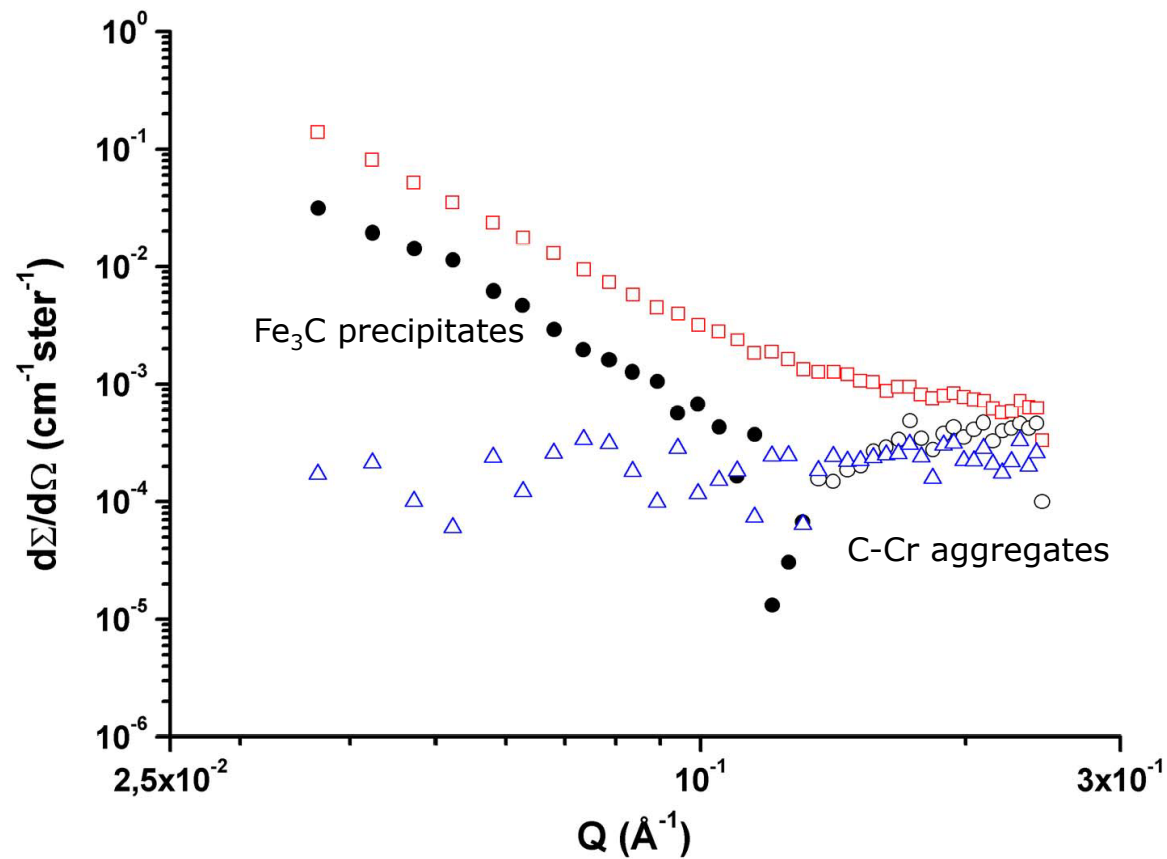
quench from 1200°



quench from 1075 °C

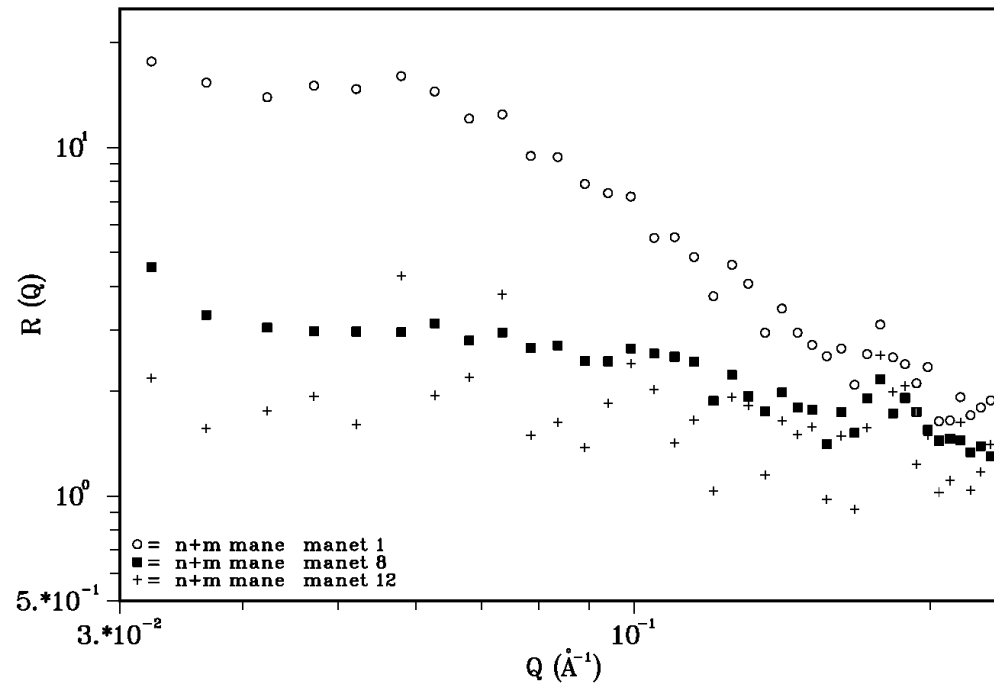
The C-Cr elementary aggregates, giving rise to the magnetic anisotropy, dissolve for $T > 1180^{\circ}\text{C}$



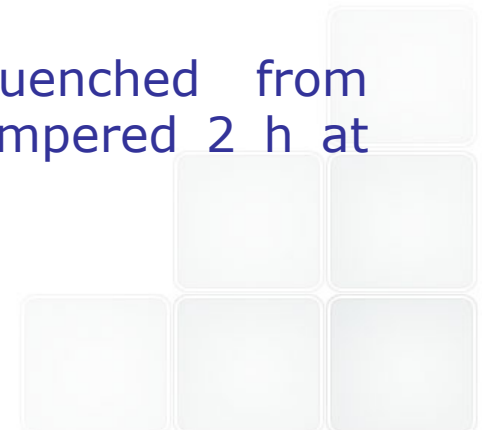


Nuclear-magnetic interference term for MANET quenched from **1075°C** (**full dots moduli of the measured negative values**, empty dots positive values), quenched from **1200°C** (triangles), quenched from 1075°C then **tempered 2 h at 700°C** (squares).

r manet1 manet8 manet12



R(Q) for MANET quenched from 1075°C (dots), quenched from 1200°C (crosses), quenched from 1075°C then tempered 2 h at 700°C (squares)



UNIRRADIATED MANET

For quench from 1075°C:

- for $Q < 10^{-1} \text{ \AA}^{-1}$ NM < 0 and $R(Q) = 10^{-11}$

precipitate phases most frequently observed in MANET steel: $M_{23}C_6$
with M standing for Fe, Cr, Fe_3C , Fe_2C or NbC

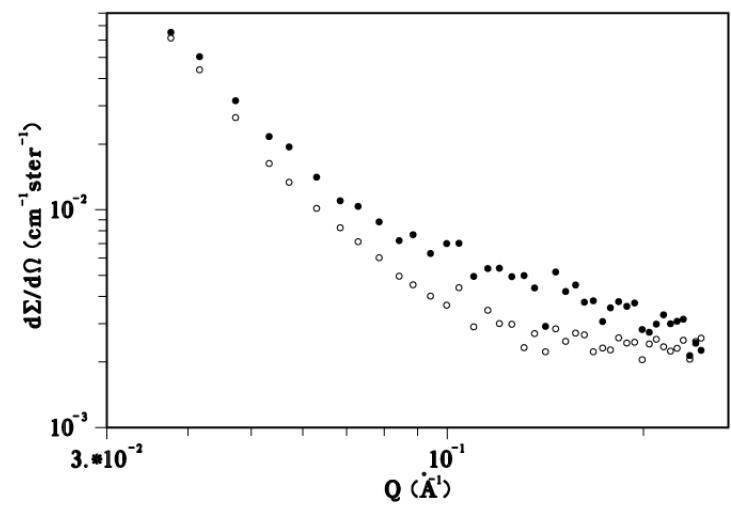
with $\rho_n^{MANET} = 7.30 \cdot 10^{10} \text{ cm}^{-2}$

$$(\Delta\rho)_n = (\rho_n^{MANET} - \rho_n^{prec.}) < 0 \Rightarrow \rho_n^{prec.} = 5.9 \text{ cm}^{-2} \quad \text{or} \\ 8.7 \cdot 10^{10} \text{ cm}^{-2} \Rightarrow$$

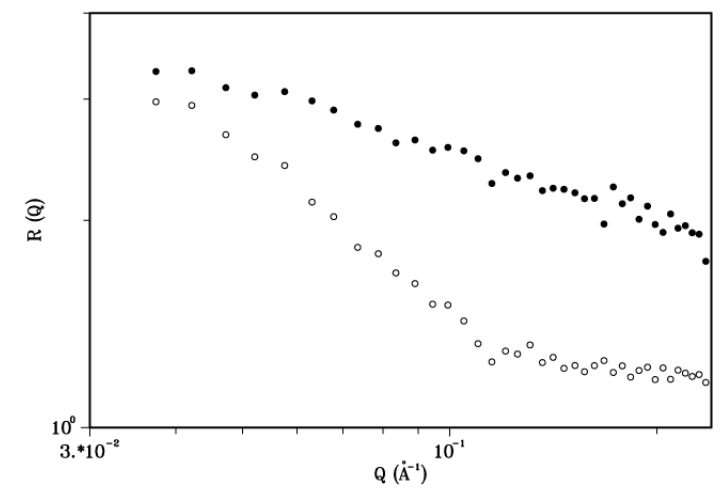
Fe_3C

- for $Q > 10^{-1} \text{ \AA}^{-1}$ (NM > 0 and $R(Q) = 2-3$) Fe is to different extents replaced by Cr (C-Cr aggregates)

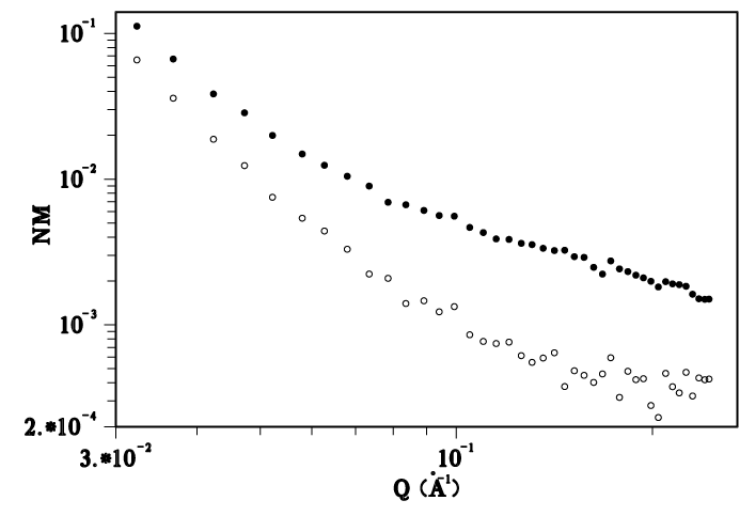
After tempering NM > 0 everywhere and $R(Q) = 1.5$ indicate that the Fe-rich precipitates dissolve and that $(Cr, Fe)_{23}C_6$ carbides grow up.



a)



b)



c)

(a) nuclear SANS cross-section N^2 for reference (empty dots) and as-irradiated (full dots) MANET samples; (b) $R(Q)$ ratio for reference (empty dots) and as-irradiated (full dots) MANET samples; (c) nuclear-magnetic interference term for reference (empty dots) and as-irradiated at 250°C 0.8 dpa (full dots) MANET.

IRRADIATED MANET

As-irradiated: increase in N , $R(Q)$ and NM with respect to reference

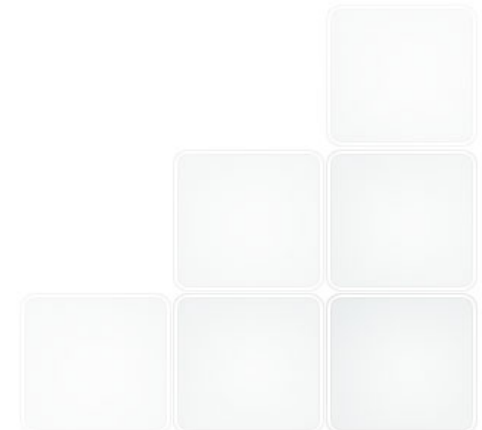
→ small magnetic defects (α' precipitates)

Irradiated and tempered: increase in N , no change in $R(Q)$ and NM with respect to reference

→ large non-magnetic defects (microvoids, He-bubbles)

Post irradiation tempering seems to promote the growth of large (1-10 nm) non-magnetic defects, such as He-bubbles or microvoids.

This effect has been observed in other irradiated steels (data analysis underway).



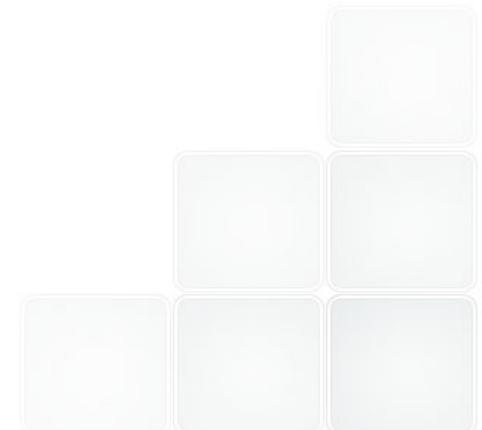
CONCLUSIONS

Polarised SANS is quite sensitive to microstructural changes in technical steels such as MANET.

The changes in N , $R(Q)$ and NM suggest the presence of small Fe-rich precipitates in the as-irradiated material while post-irradiation tempering promotes the growth of microvoids or He-bubbles.

This method appears therefore extremely promising and is being applied to several other steels (with different compositions).

A wider Q -range as well as more detailed TEM information are necessary for more quantitative interpretation.



REFERENCES

- R. Coppola, R. Kampmann, M. Magnani, P. Staron, *Microstructural investigation, using polarized neutron scattering, of a martensitic steel for fusion reactors*, Acta mat. 46 (1998) 5447
- R. Coppola, C. D. Dewhurst, R. Lindau, R. P. May, A. Möslang, M. Valli, *Polarised SANS study of microstructural evolution under neutron irradiation in a martensitic steel for fusion reactors*, Physica B 345 (2004) 225
- R. Coppola, M. Klimiankou, R. Lindau, A. Möslang, M. Valli, *Helium-bubble evolution in F82H mod – Correlation between SANS and TEM*, J. N. M. 329-333 (2004) 1057
- R. Coppola, R. Lindau, M. Magnani, R. P. May, A. Möslang, J. W. Rensman, B. van der Schaaf, M. Valli, *Microstructural investigation, using SANS, of neutron irradiated Eurofer97 steel*, F. Eng. & Des. 75-79 (2005) 985
- R. Coppola, R. Lindau, R. P. May, A. Möslang, M. Valli, *Investigation of microstructural evolution under neutron irradiation in Eurofer97 steel by means of small-angle neutron scattering*, J. Nucl. Mat. 386-388 (2009) 195-198
- R. Coppola, R. Lindau, A. Möslang, M. Valli, A. Wiedenmann, *Recent applications of small-angle neutron scattering in the characterisation of irradiated steels for nuclear technology*, pres. at EC-IAEA Workshop, Barcelona October 2009 J. Nucl. Mat. 409 (2011) 100